

Dielectrophoretic Rayleigh-Bénard convection under microgravity conditions

H. N. Yoshikawa,* M. Tadie Fogaing, O. Crumeyrolle, and I. Mutabazi

Laboratoire Ondes et Milieux Complexes, UMR 6294 CNRS, Université du Havre, 53, rue de Prony, CS80540, 76058 Le Havre Cedex, France

(Received 24 December 2012; published 8 April 2013)

Thermal convection in a dielectric fluid layer between two parallel plates subjected to an alternating electric field and a temperature gradient is investigated under microgravity conditions. A thermoelectric coupling resulting from the thermal variation of the electric permittivity of the fluid produces the dielectrophoretic (DEP) body force, which can be regarded as thermal buoyancy due to an effective gravity. This electric gravity can destabilize a stationary conductive state of the fluid to develop convection. The similarity of the DEP thermal convection with the Rayleigh-Bénard (RB) convection is examined by considering its behavior in detail by a linear stability theory and a two-dimensional direct numerical simulation. The results are analyzed from an energetic viewpoint and in the framework of the Ginzburg-Landau (GL) equation. The stabilizing effects of a thermoelectric feedback make the critical parameters different from those in the RB instability. The nonuniformity of the electric gravity arising from the finite variation of permittivity also affects the critical parameters. The characteristic constants of the GL equation are comparable with those for the RB convection. The heat transfer in the DEP convection is weaker than in the RB convection as a consequence of the feedback that impedes the convection.

DOI: [10.1103/PhysRevE.87.043003](https://doi.org/10.1103/PhysRevE.87.043003)

PACS number(s): 44.25.+f, 47.65.-d

I. INTRODUCTION

The application of an electric field \mathbf{E} on a dielectric fluid gives rise to the electrohydrodynamic force density \mathbf{f}_{EHD} [1]:

$$\mathbf{f}_{\text{EHD}} = \rho_f \mathbf{E} - \frac{1}{2} E^2 \nabla \epsilon + \nabla \left[\frac{\rho}{2} \left(\frac{\partial \epsilon}{\partial \rho} \right)_T E^2 \right], \quad (1)$$

where ρ_f is the free electric charge density, E is the magnitude of \mathbf{E} , and T is the temperature. The electric permittivity and mass density of the fluid are denoted by ϵ and ρ , respectively. The first term is the electrophoretic force arising from the Coulomb forces that the field exerts on free charges. It is often the dominant component of \mathbf{f}_{EHD} under a static or low-frequency electric field. When the frequency f is high compared with the viscous time scale $\tau_v = d^2/\nu$ (d is the length scale of a flow and ν is the kinematic viscosity of the fluid), the fluid cannot respond to the rapid variation of \mathbf{E} and the electrophoretic force has no influence on its motion, as long as the charge density ρ_f does not vary over the period f^{-1} . Under such a high-frequency electric field, the second term of Eq. (1), called the dielectrophoretic (DEP) force, becomes dominant, as E^2 has a static component. The third term is an electrostrictive force which would not influence flows when the fluid is incompressible and has no mobile boundaries [2].

The DEP force can arise when the fluid is subjected to a temperature gradient. The electric permittivity ϵ is a decreasing function of the temperature in the most of dielectric fluids and can be modeled by a linear relationship:

$$\epsilon(\theta) = \epsilon_1(1 - e\theta), \quad (2)$$

where ϵ_1 is the electric permittivity at a reference temperature T_1 and θ is the temperature deviation from the reference temperature: $\theta = T - T_1$. A temperature gradient then results in a DEP force directed from low- to high-temperature regions in the fluid. This thermoelectric force can generate a thermal

convection, and, hence, it can be used to enhance heat transfer in dielectric fluids even under microgravity conditions.

The electric gravity \mathbf{g}_e is often employed in the analysis of the DEP thermal convection for its intuitive comprehension. With use of Eq. (2), the DEP force can be developed as $-E^2 \nabla \epsilon / 2 = \nabla(e\theta \epsilon_1 E^2 / 2) - \theta e \nabla(\epsilon_1 E^2 / 2)$. The first term is a gradient force that can be lumped with the pressure term in the dynamical equations of fluid motion. The second term can be regarded as a thermal buoyancy force, $-\rho \alpha \theta \mathbf{g}_e$ (α is the coefficient of thermal expansion), due to an effective gravity \mathbf{g}_e :

$$\mathbf{g}_e = \frac{e}{\alpha \rho} \nabla \left(\frac{\epsilon_1 E^2}{2} \right), \quad (3)$$

which represents the variation of the electric energy stored in the dielectric fluid per volume. This electric gravity varies in space and time in general. The electric Rayleigh number $L = \alpha \Delta \theta g_{e0} d^3 / \kappa \nu$ is then introduced as control parameter of the DEP thermal convection, where g_{e0} is the characteristic value of the electric gravity (d and $\Delta \theta$ are the gap and the temperature difference between the electrodes, κ is the thermal diffusivity).

Roberts [3], Turnbull [4], and Stiles [5] have investigated the linear stability of a horizontal fluid layer between two parallel plane electrodes kept at different temperatures. Under the assumption that the DEP force was the primary component of the electrohydrodynamic force, they found its destabilizing effects on the stationary conductive state. Convection developed beyond critical values L_c of the electric Rayleigh number, even in ordinarily stable thermal stratification where the temperature gradient was directed upwards. Under microgravity conditions, it was found that $L_c = 2128.7$ with the critical wave number $k_c = 3.226/d$. Takashima and Hamabata [6] have considered the same problem but in a vertical configuration of electrodes, assuming a vertical basic flow in the conductive regime. Instability occurred in different modes: hydrodynamic, thermal, and electric, depending on the values of L and the Grashof number Gr . In the limit of small Gr , the electric mode instability appeared at the same L_c and k_c

*harunori.yoshikawa@univ-lehavre.fr

as those in microgravity. The DEP convection in its nonlinear regime has not been investigated so much. Stiles *et al.* [7] have performed a weakly nonlinear analysis. They have estimated the heat transfer enhancement by convection for a Prandtl number $\text{Pr} (= \nu/\kappa) = 10$ and found $\text{Nu} - 1 \approx 0.8(L/L_c - 1)$ in the vicinity of the criticality.

The similarity of the DEP thermal convection with the ordinary thermal convections has been noticed for a long time. However, the above critical parameters and Nusselt number are different from those in the RB convection. These differences have never been explained to the authors' knowledge. Furthermore, the DEP convection involves a parameter $\gamma_e = e\Delta\theta$ which has no corresponding part in the RB convection. This dimensionless permittivity variation γ_e has been assumed to be small: $|\gamma_e| \ll 1$ in the previous theoretical works [3,5–7], although it can be significant in some dielectric fluids with a large thermal coefficient e , e.g., in acetonitrile and nitrobenzene, $e \approx 0.2$.

In the present work, we examine the similarity of the DEP thermal convection in plane geometry with the RB convection by detailed theoretical considerations. We perform a linear stability analysis in a system with an infinite lateral extension, taking into account finite values of γ_e . A two-dimensional direct numerical simulation for a system with a large aspect ratio is also carried out for different $\text{Pr} (\geq 1)$ to investigate the nonlinear behavior of the convection. Obtained results are analyzed from an energetic viewpoint and in the framework of the Ginzburg-Landau equation.

The governing equations of the DEP thermal convection are given in Sec. II with the basic conductive state. An energy equation is also given there for later discussions. The linear stability theory and its results are presented in Sec. III. The results of the direct numerical simulation are given in Sec. IV with their analysis by the Ginzburg-Landau (GL) equation. The heat transfer enhancement is also discussed. The final section gives our conclusions.

II. PROBLEM FORMULATION

A. Governing equations

A dielectric fluid layer subjected to an alternating electric voltage $\sqrt{2}V_0 \sin(2\pi ft)$ and to a temperature difference $\Delta\theta$ is considered (Fig. 1). For an electric field with a high frequency compared to the viscous time scale τ_ν , only the time-averaged component of the DEP force can induce the convective motion of the fluid [8,9]. In this high-frequency approximation, the equations of continuity, of motion, and of heat conduction and Gauss's law of electricity read in the electrohydrodynamic

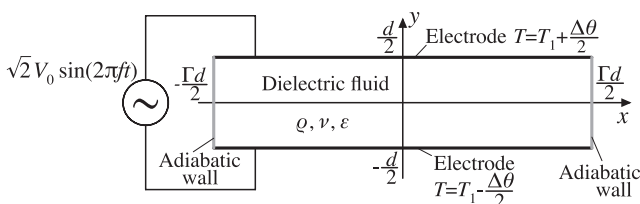


FIG. 1. Geometrical configuration of the problem.

Boussinesq approximation [8]:

$$\nabla \cdot \mathbf{u} = 0, \quad (4)$$

$$\partial_t \mathbf{u} + \mathbf{u} \cdot \nabla \mathbf{u} = -\nabla \pi + \nabla^2 \mathbf{u} - \frac{L}{\text{Pr}} \theta \mathbf{g}_e, \quad (5)$$

$$\partial_t \theta + \mathbf{u} \cdot \nabla \theta = \frac{1}{\text{Pr}} \nabla^2 \theta, \quad (6)$$

$$\nabla \cdot [\epsilon(\theta) \nabla \phi] = 0 \quad \text{with} \quad \mathbf{E} = -\nabla \phi \quad (7)$$

where \mathbf{u} is the two-dimensional velocity field: $\mathbf{u} = u\hat{x} + v\hat{y}$ (\hat{x} , \hat{y} being the unit vectors along the x and y axes), π is the generalized pressure including electrohydrodynamic components, and ϕ is the electric potential. The equations have been nondimensionalized with scales d of length, d^2/ν of time, V_0 of electric potential, and $\Delta\theta$ of temperature. In the present study the scale of time d^2/ν is more appropriate than the time scale of thermal diffusion d^2/κ , as the former is the smallest when $\text{Pr} > 1$, the case in which we are interested. The permittivity is scaled by ϵ_1 and its thermal variation is given by $\epsilon = 1 - \gamma_e \theta$ according to Eq. (2).

These equations are completed by the boundary conditions on the electrodes at $y = \pm 1/2$ and on the walls at $x = \pm \Gamma/2$ (Γ : the aspect ratio):

$$\mathbf{u} = 0, \quad \theta = \frac{1}{2}, \quad \phi = 1 \quad \text{at} \quad y = -\frac{1}{2}, \quad (8)$$

$$\mathbf{u} = 0, \quad \theta = -\frac{1}{2}, \quad \phi = 0 \quad \text{at} \quad y = \frac{1}{2}, \quad (9)$$

$$\mathbf{u} = 0, \quad \partial_x \theta = 0, \quad \partial_x \phi = 0 \quad \text{at} \quad x = \pm \frac{\Gamma}{2}. \quad (10)$$

We have assumed that the walls are thermally adiabatic and made of a material with a small electric permittivity compared to the fluid [Eq. (10)], considering the problem in its simplest configuration.

In the theoretical model formulated by Eqs. (4)–(10), we have considered an initially electroneutral fluid layer and have assumed that no space charge accumulation is induced by the electric field: $\rho_f = 0$ in the bulk of the fluid during the entire development of convection flow. This assumption is valid under the following conditions: (i) $f \gg \tau_e^{-1}, \tau_m^{-1}, \tau_d^{-1}$ and (ii) $d \gg \lambda_D$, where τ_e , τ_m , and τ_d are the time scales of the charge relaxation, migration, and diffusion processes, respectively. The Debye length λ_D represents the thickness of the diffusion layer, which is an electrically charged layer constituting the outer part of the electric double layer formed on each fluid-electrode interface. Under condition (i), the electric field varies too rapidly to alter the spatial distribution of charges in the fluid; under condition (ii), the charge transport by the convection flows from the diffusion layer into the bulk will be negligible.

For a bipolar system consisting of positive and negative charges of the same magnitude q , the time scales and the Debye length are given by [10]

$$\tau_e = \frac{\epsilon}{\sigma}, \quad \tau_m = \frac{h}{E(b_+ + b_-)}, \quad \tau_d = \frac{h^2}{\frac{K_+ b_- + K_- b_+}{b_+ + b_-}},$$

$$\lambda_D = \sqrt{\frac{\epsilon k_B T}{2q^2 n_\infty}}, \quad (11)$$

where σ is the electric conductivity, h is a length scale, k_B is the Boltzmann constant, n_∞ is the number density of both charges far from electrodes, and b_\pm and K_\pm are, respectively, the mobilities and diffusion coefficients of positive and negative charges. In silicone oils, the time scales are estimated for the diffusion layer (i.e., $h = \lambda_D$) as $\tau_e \sim 10\text{--}10^2$ s, $\tau_d \sim 10^2$ s, and $\tau_m \sim 8.2 \times 10^6 \nu^{1/2} E^{-1} (q/q_e)^{-1/2}$ [s] with $\lambda_D \sim 10^{-4}$ m, where q_e is the elementary charge and ν and E are their values in the units of m^2/s and V/m , respectively [11]. The migration time τ_m gives the smallest value among the three time scales at practical field strengths ($E \sim 10^5\text{--}10^6$ V/m), being, e.g., $\tau_m = 0.026$ s for a silicone oil with $\nu = 10^{-5}$ m^2/s . According to conditions (i) and (ii), the theoretical model (4)–(10) would enable one to describe the flow in a layer of the latter oil, thicker than a few millimeters and subjected to an electric field with a frequency higher than $\tau_m^{-1} = 38$ Hz.

B. Conductive state

When the imposed temperature difference is small, the purely conductive state ($\mathbf{u} = 0$) is established. The temperature and electric fields, $\theta = \bar{\theta}(y)$ and $\phi = \bar{\phi}(y)$, are then obtained analytically from Eqs. (6) and (7) with the boundary conditions (8)–(10):

$$\bar{\phi} = \frac{\log\left(\frac{1+\gamma_e y}{1+\gamma_e/2}\right)}{\log\left(\frac{1-\gamma_e/2}{1+\gamma_e/2}\right)}, \quad \bar{\theta} = -y. \quad (12)$$

This conductive state is independent of the aspect ratio Γ due to the idealized boundary condition (10). It will therefore be considered as the basic state both in the linear stability theory performed for $\Gamma \rightarrow \infty$ and in the DNS for a large but finite Γ . The electric gravity (3) in the conductive state is given by

$$\bar{\mathbf{g}}_e = \bar{g}_e \hat{\mathbf{y}} \quad \text{with} \quad \bar{g}_e = -\frac{1}{(1+\gamma_e y)^3}. \quad (13)$$

We have chosen for scaling $\bar{\mathbf{g}}_e$ the electric gravity at the middle of the gap: $g_{e0} = e\epsilon_1 V_0^2 \gamma_e^3 / \rho \alpha d^3 [\log\{(1-\gamma_e/2)/(1+\gamma_e/2)\}]^2$. The electric Rayleigh number L in Eq. (5) is based on the characteristic gravity g_{e0} :

$$L = \frac{\epsilon_1 V_0^2 \gamma_e^4}{\rho \kappa \nu} \left[\log\left(\frac{1-\gamma_e/2}{1+\gamma_e/2}\right) \right]^{-2}, \quad (14)$$

which recovers the electric Rayleigh number introduced in the previous works [3,5–7] in the limit of small γ_e .

C. Energy equation

An equation that governs the evolution of the flow kinetic energy can be derived from the Navier-Stokes equation (5). Taking the inner product of the equation with \mathbf{u} and integrating over the whole fluid domain, we have

$$\frac{dK}{dt} = W_{BG} + W_{PG} - D_v, \quad (15)$$

where K , W_{BG} , W_{PG} , and D_v are the flow kinetic energy, the work done by the basic electric gravity $\bar{\mathbf{g}}_e$, the work done by the perturbation electric gravity $\mathbf{g}'_e = \mathbf{g}_e - \bar{\mathbf{g}}_e$, and the viscous dissipation, respectively. They are computed by integrating over the fluid domain the corresponding quantities per

volume:

$$\mathcal{K} = |\mathbf{u}'|^2/2, \quad (16)$$

$$w_{BG} = -\text{Pr}^{-1} L \theta' \mathbf{u}' \cdot \bar{\mathbf{g}}_e, \quad (17)$$

$$w_{PG} = -\text{Pr}^{-1} L (\bar{\theta} \mathbf{u}' \cdot \mathbf{g}'_e + \theta' \mathbf{u}' \cdot \mathbf{g}'_e), \quad (18)$$

$$d_v = \nabla \mathbf{u}' : (\nabla \mathbf{u}')^T, \quad (19)$$

where the primes indicate perturbation quantities.

The basic electric gravity $\bar{\mathbf{g}}_e$ can be regarded as the counterpart in the DEP thermal convection to the Earth's gravity in the ordinary thermal convections. The perturbation electric gravity \mathbf{g}'_e represents a thermoelectric feedback associated with the electric field perturbations that arise from temperature disturbances [Eq. (7)]. The contribution of the work W_{PG} to the kinetic energy evolution is hence distinctive of the DEP convection.

III. LINEAR STABILITY THEORY

Governing equations (4)–(7) are linearized about the basic state (12). Developing perturbations into normal modes e^{st+ikx} with the complex growth rate s and the wave number k , we have

$$0 = ikU + DV, \quad (20)$$

$$sU = (D^2 - k^2)U - ik\Pi - \frac{L}{\text{Pr}} \bar{\theta} G_{ex}, \quad (21)$$

$$sV = (D^2 - k^2)V - D\Pi - \frac{L}{\text{Pr}} \bar{g}_e \Theta - \frac{L}{\text{Pr}} \bar{\theta} G_{ey}, \quad (22)$$

$$s\Theta = V + \frac{1}{\text{Pr}} (D^2 - k^2)\Theta, \quad (23)$$

$$0 = -\gamma_e [D\bar{\phi}D + D^2\bar{\phi}]\Theta + [(1+\gamma_e y)(D^2 - k^2) + \gamma_e D]\Phi, \quad (24)$$

where (U, V, Π, Θ, Φ) are the normal mode amplitudes of the perturbations ($u', v', \pi', \theta', \phi'$), respectively, and the operator $D = d/dy$. The normal mode amplitudes (G_{ex}, G_{ey}) of the perturbation electric gravity \mathbf{g}'_e are given by

$$\begin{aligned} G_{ex} \hat{\mathbf{x}} + G_{ey} \hat{\mathbf{y}} &= \frac{1}{\gamma_e^3} \left[\log\left(\frac{1-\gamma_e/2}{1+\gamma_e/2}\right) \right]^2 \\ &\times [ikD\bar{\phi}D\Phi \hat{\mathbf{x}} + (D\bar{\phi}D^2\Phi + D^2\bar{\phi}D\Phi) \hat{\mathbf{y}}]. \end{aligned} \quad (25)$$

On the electrodes the perturbations satisfy the following boundary conditions corresponding to Eqs. (8) and (9):

$$U = DU = V = \Theta = \Phi = 0 \quad \text{at} \quad y = \pm \frac{1}{2}. \quad (26)$$

The condition on the adiabatic walls (10) has been removed, as we consider a system with an infinite lateral extension ($\Gamma \rightarrow \infty$) in the present linear theory.

The set of equations (20)–(24) are discretized by a spectral collocation method. All the unknown functions are developed into Chebyshev series, and the equations are considered only at the Chebyshev-Gauss-Lobatto collocation points. The highest order of considered Chebyshev polynomials is set at 60 to ensure the convergence. The discretized governing equations

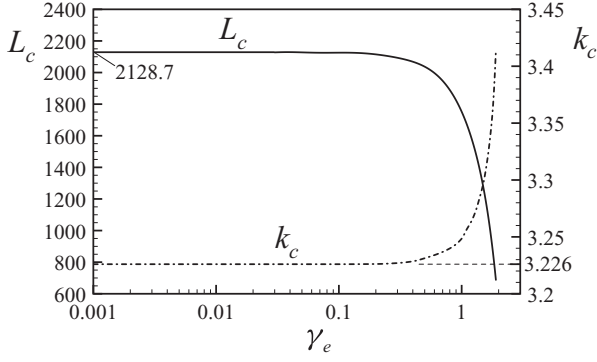


FIG. 2. Critical values of the electric Rayleigh number L and the wave number k as functions of the thermal variation of electric permittivity γ_e . The predictions of the previous linear stability theories ($L_c = 2128.7$, $k_c = 3.226$) [3,5,6] are indicated for comparison.

are coupled with the boundary conditions (26) to form a generalized eigenvalue problem. Its eigenvalues and eigenvectors are computed by employing the QZ decomposition.

Marginal stability curves are obtained by solving the eigenvalue problem for different values of L and k at given Pr and γ_e . The minimum of a marginal curve gives the critical parameters (k_c, L_c), which are found to be independent of the Prandtl number. The corresponding critical mode is stationary as in the RB problem [12,13]. The critical parameters for small γ_e (<0.1) are constant, recovering the results of the existing theories [3,5,6]. For large γ_e (>0.1), the critical parameters depend on it (Fig. 2): significant decrease and increase are found in L_c and k_c , respectively.

The basic electric gravity \bar{g}_e provides energy to perturbation flow, i.e., $W_{BG} > 0$ (Fig. 3). The mechanism driving the convection is hence the thermal buoyancy associated with a temperature perturbation θ' in the gravity \bar{g}_e , similar to the RB instability. In contrast, the perturbation gravity \bar{g}'_e dissipates energy, $W_{PG} < 0$ (Fig. 3). This stabilization by \bar{g}'_e is absent in the RB convection and explains why L_c at small γ_e is larger than the critical Rayleigh number R_c ($=1708$) in the RB convection in spite of the apparent similarity in the driving mechanism. The effect of W_{PG} is also found to

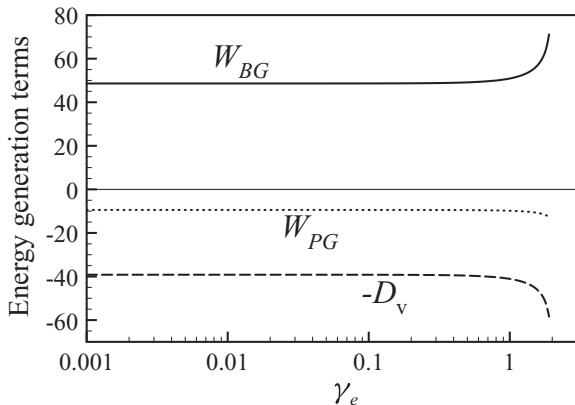


FIG. 3. Different terms in the energy equation (15) at critical conditions. The work done by the basic electric gravity W_{BG} , the work done by the perturbation electric gravity W_{PG} , and the viscous dissipation D_v are all normalized by twice the kinetic energy K .

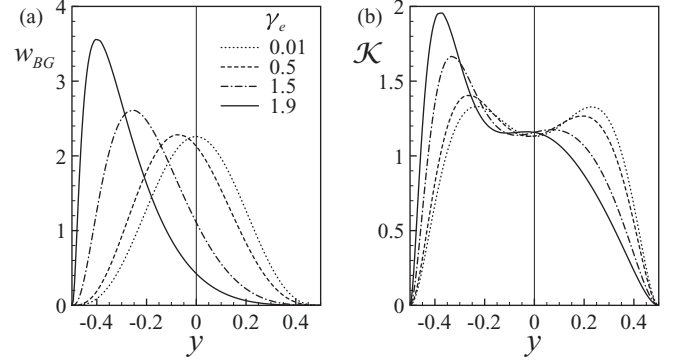


FIG. 4. Profiles of the local work done by the basic electric gravity w_{BG} and the local flow kinetic energy \mathcal{K} , averaged along the x direction and normalized, respectively, by W_{BG} and K .

be more significant at small wave number, giving an explanation to $k_c = 3.226$ that is larger than in the RB instability ($k_c = 3.117$).

For large γ_e , the work W_{BG} is enhanced, although the work W_{PG} is almost constant (Fig. 3). This suggests that the basic electric gravity performs work more efficiently at large γ_e than at small γ_e to destabilize the conductive state at small L_c . Indeed, the spatial nonuniformity of the basic electric gravity \bar{g}_e is reinforced at large γ_e [Eq. (13)] and strong electric gravity in the vicinity of the hot electrode ($y = -\frac{1}{2}$) provides energy to the fluid locally [Fig. 4(a)]. The instability is then provoked within a fluid sublayer attached to the electrode. As a consequence, the kinetic energy of developed flow is also concentrated in the region near the hot electrode [Fig. 4(b)]: The convection develops within an effective sublayer of a small thickness. This explains the observed large critical wave numbers (i.e., small wavelengths) at large γ_e .

IV. DIRECT NUMERICAL SIMULATION

We have considered the nonlinear behavior of the DEP thermal convection for a small γ_e ($=0.03$) and a large aspect ratio $\Gamma = 114$, solving the set of partial differential equations (4)–(7) with the boundary conditions (8)–(10) by the finite element method implemented in a commercial software package (COMSOL Multiphysics 3.5, Comsol AB, Stockholm, Sweden). Numerical grids are made of identical rectangles with sides of $\Delta x = 0.15$ and $\Delta y = 0.1$ so that the fluid domain is divided by 760 and 10 along the x and y directions, respectively. The backward differentiation formula is used for the time integration. The convergence of computation was verified by grid refinements. The initial fields are specified as null for the velocities, the temperature, and the electric field: The solved problem corresponds to a situation where the electric potential V_0 and the temperature difference $\Delta\theta$ are imposed instantaneously on a steady isothermal fluid layer at $t = 0$.

For a value of L larger than L_c , small disturbances grow exponentially to develop convection cells. This linear growth stage is followed by a saturation where hot and cold cells are shifted toward the low- and high-temperature electrodes, respectively, yielding a net heat transfer enhancement by the convection [Figs. 5(a) and 5(b)]. The cells have a well-defined

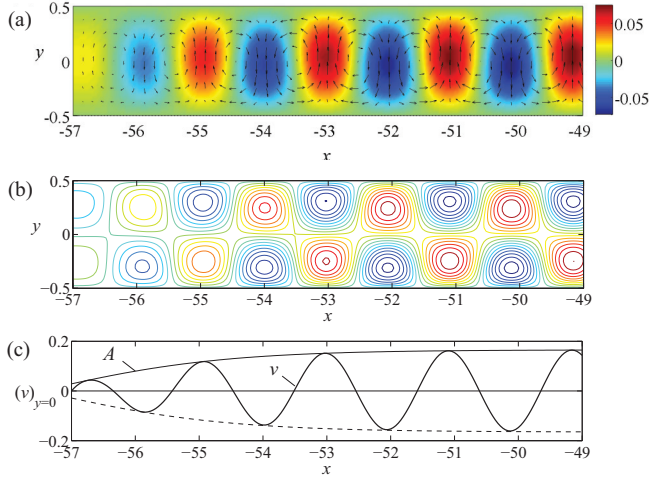


FIG. 5. (Color online) Convection flow in the saturated state for $Pr = 10$ at $L = 2200$: (a) velocity (arrows) and perturbation temperature (color), (b) equipotentials of perturbation electric field, and (c) the profile of the transversal velocity component v at the middle of the gap ($y = 0$). The left end ($x = -57$) corresponds to one of the adiabatic lateral walls.

wave number k along the x direction. Its Fourier spectrum has a sharp peak with a width around $\Delta k = 0.05$ arising from the perturbation suppression at the lateral walls.

A. Description by the Ginzburg-Landau equation

The bifurcation at $L = L_c$ is found to be supercritical. As the critical mode is stationary and has a finite wave number k_c (i.e., Type I-s instability [14]), the behavior of the perturbation amplitude in the weakly nonlinear regime is hence expected to be described by the Ginzburg-Landau (GL) equation:

$$\tau_0 \partial_t A = \delta A + \xi_0^2 \partial_x^2 A - \ell |A|^2 A, \quad (27)$$

where δ is the supercriticality $\delta = L/L_c - 1$. The constants τ_0 , ξ_0 , and ℓ are characteristics of a given system. In the present work, the envelope of the velocity profile $v = v(x)$ at the middle of the gap ($y = 0$) will be taken as the amplitude A .

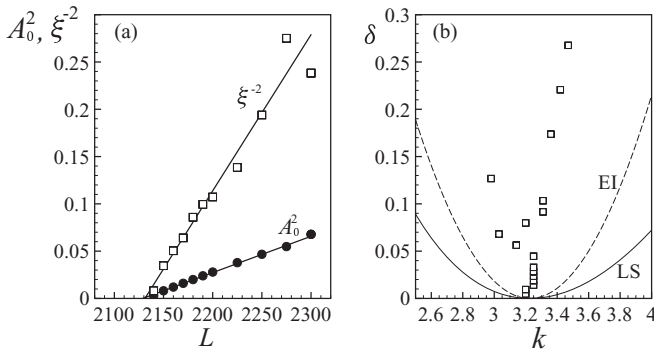


FIG. 6. Behavior of (a) the healing length ξ and the saturation amplitude A_0 and (b) the wave number k in the vicinity of the criticality ($Pr = 10$). The supercriticality $\delta (=L/L_c - 1)$ is computed with $L_c = 2130$. (b) Also shown are the marginal curve obtained in the linear stability theory (LS) and the Eckhaus instability boundary (EI): $\delta = 3\xi_0^2(k - k_c)^2$.

TABLE I. Critical parameters and characteristic constants of the Ginzburg-Landau equation (27) determined from the DNS ($\gamma_e = 0.03$).

Pr	L_c	τ_0	ξ_0	ℓ
1	2128.2	0.0783	0.388	0.0121
10	2128.9	0.590	0.377	1.15
100	2130.1	5.62	0.380	118
1000	2130.0	55.9	0.381	11 800

In the saturated state, the amplitude is constant far from the adiabatic walls [Fig. 5(c)] where the GL equation predicts $|A| = \sqrt{\delta/\ell} = \sqrt{(L/L_c - 1)/\ell} (=A_0)$. The critical electric Rayleigh number L_c can be deduced from the intersection point of the A_0^2 line with the L axis [Fig. 6(a)]. We find $L_c = 2130$, independent from the Prandtl number (Table I) as in the linear stability theories [3,4,6,7]. The perturbation suppression by the lateral walls affects the critical parameters little, since the aspect ratio Γ is large.

In a large system, the solution of the GL equation in the vicinity of a suppressing lateral boundary is given by $A = e^{i\Phi} \sqrt{\delta/\ell} \tanh[(x - x_w)/\xi]$. On the first order, x_w is identical to the wall position, and the phase Φ is an arbitrary constant. The constant ξ represents a distance over which perturbations heal from the suppression at the boundary and is given by $\xi = \sqrt{2}\xi_0\delta^{-1/2}$. The hyperbolic tangent is a correct envelope function of $(v)_{y=0}$ [Fig. 5(c)]. The determined healing length ξ behaves as the theoretical predictions: ξ^{-2} increases linearly with L and intersects the L axis at $L = L_c$ [Fig. 6(a)].

The values of the characteristic constants τ_0 , ξ_0 , and ℓ were found from the linear fits for δ/τ_0 (the growth rate), ξ^{-2} , and A_0^2 as functions of the supercriticality δ . Table I shows the determined values of the constants for different values of Pr . The characteristic time τ_0 increases linearly with Pr and can be correlated by the same relationship derived for the RB convection: $\tau_0 = (Pr + 0.5117)/19.65$ [15]. The values of ξ_0 do not vary with Pr and are also identical to the value found in the RB problem: $\xi_0 = 0.385$. The determined ξ_0 enables us to draw the stability boundary of the Eckhaus instability: $\delta = 3\xi_0^2(k - k_c)^2$ [Fig. 6(b)]. The wave numbers obtained in the DNS are inside the stable zone. The constant ℓ behaves as $\ell \propto Pr^2$, implying $|A| \propto Pr^{-1}$. Since we have chosen the

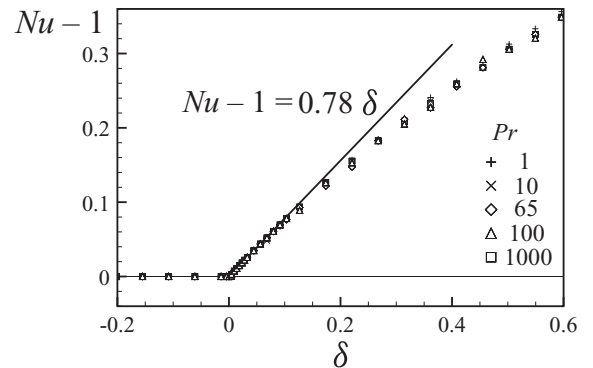


FIG. 7. Heat transfer enhancement by saturated convection flows. The Nusselt number Nu is shown as a function of the supercriticality δ for different Prandtl numbers Pr ($\gamma_e = 0.03$).

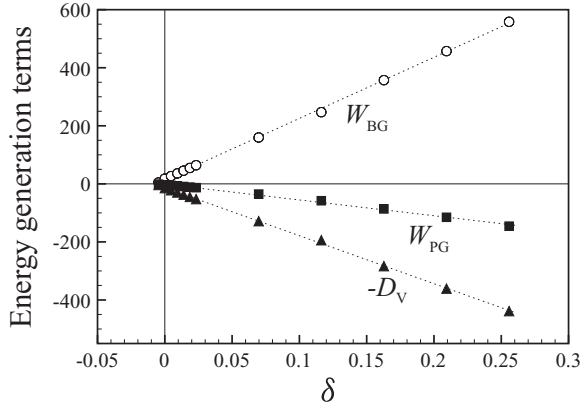


FIG. 8. Different terms in the energy equation (15) in the vicinity of the criticality in saturated states ($\text{Pr} = 10$). The work done by the basic electric gravity W_{BG} , the work done by the perturbation electric gravity W_{PG} , and the viscous dissipation D_v are all normalized by twice the kinetic energy K .

envelope of the velocity v as the amplitude A , this means that the convection velocity is scaled by $\text{Pr}^{-1}(v/d) = \kappa/d$, as in the ordinary thermal convections.

B. Heat transfer enhancement

The heat transfer is enhanced by the developed convection for $L > L_c$. Figure 7 shows the Nusselt number Nu as a function of the supercriticality δ :

$$\text{Nu} = \frac{1}{\Gamma} \left(- \int_{-\Gamma/2}^{\Gamma/2} \partial_y \theta dx + \text{Pr} \int_{-\Gamma/2}^{\Gamma/2} v \theta dx \right). \quad (28)$$

This number is the ratio of the total heat transfer to the conductive heat transfer in the basic state (12). The behavior of Nu is correlated by $\text{Nu} - 1 = 0.78\delta$ [16] for small supercriticality δ , independent of the Prandtl number Pr (≥ 1). The coefficient 0.78 agrees with its value obtained in a weakly nonlinear analysis for $\text{Pr} = 10$ [7].

In the RB convection, the relationship $\text{Nu} - 1 \approx 1.43(R/R_c - 1)$ [17] has been found for steady roll modes for $\text{Pr} > 1$. The coefficient of the supercriticality found for the DEP convection is hence substantially smaller than in the RB convection. This difference is too large to be explained by the spatial nonuniformity of the basic gravity (13) or by the presence of the lateral walls: The former effect will be of the order of $O(\gamma_e) = 10^{-2}$ and the latter one will be about $O(\Gamma^{-1}) = 10^{-2}$. In the linear stability theory, it was found that \mathbf{g}'_e tends to dissipate the kinetic energy of flow (Fig. 3). This tendency persists even after the saturation (Fig. 8). The reduction in convective heat transfer by the perturbation elec-

tric gravity will be of the order of $W_{PG}/W_{BG} \approx 0.3$, agreeing with the relative difference between the coefficients in the Nu correlations. The impeding effect of the perturbation electric gravity \mathbf{g}'_e on convection flows hence gives an explanation to the weaker heat transfer enhancement in the DEP convection than in the RB convection.

V. CONCLUSIONS

In the present study, the similarity of the DEP thermal convection in plane geometry with the RB convection has been examined in detail by a linear stability analysis and a direct numerical simulation. The problem was formulated with regarding the DEP force as thermal buoyancy due to the electric gravity (3). The difference from the RB convection was highlighted by introducing the perturbation electric gravity \mathbf{g}'_e , which represents the thermoelectric feedback, and by considering finite values of the permittivity variation γ_e , which is associated with the nonuniformity in the basic gravity $\bar{\mathbf{g}}_e$ [Eq. (13)].

The linear stability theory revealed that the electric gravity perturbation dissipates flow kinetic energy and tends to stabilize the basic conductive state. The critical parameters L_c and k_c are hence different from those of the RB instability even when $\bar{\mathbf{g}}_e$ is almost uniform over the gap. When the nonuniformity of $\bar{\mathbf{g}}_e$ is important ($\gamma_e > 0.1$), the instability occurs within a fluid sublayer attached on the hot electrode where the electric gravity is strong and provides energy efficiently to convective flows. As a consequence, the critical values of L and k decrease and increase, respectively, from their values at small γ_e .

The results obtained by the DNS showed that the convection develops when $L > L_c$ with wave numbers inside the Eckhaus stable zone. The convection flow in the nonlinear regime is well described by the GL equation. The determined characteristic time τ_0 increases with Pr in the same manner as that obtained for the RB convection. The characteristic length ξ_0 is constant, being also the same as that in the RB convection. In spite of this similarity, impeding effects of the perturbation electric gravity persist in the nonlinear regime and result in a heat transfer enhancement weaker than in the RB convection.

ACKNOWLEDGMENTS

This work has benefited from partial financial support from the CNES (Centre National des Etudes Spatiales). M.T.F. was supported by the doctor scholarship from the French Ministry of Higher Education and Research. H.N.Y. wishes to thank the Université du Havre and the FEDER (Fonds Européen de Développement Régional) for support through a postdoctoral grant. The authors have had enriching discussions during the GEOFLOW Topical Team Meetings in Cottbus.

[1] L. D. Landau and E. M. Lifshitz, *Electrodynamics of Continuous Media*, 2nd ed., Landau and Lifshitz Course of Theoretical Physics, Vol. 8 (Elsevier Butterworth-Heinemann, Burlington, MA, 1984).

[2] T. B. Jones, *Adv. Heat Transfer* **14**, 107 (1979).

[3] P. H. Roberts, *Q. J. Mech. Appl. Math.* **22**, 211 (1969).

[4] R. J. Turnbull, *Phys. Fluids* **12**, 1809 (1969).

[5] P. J. Stiles, *Chem. Phys. Lett.* **179**, 311 (1991).

- [6] M. Takashima and H. Hamabata, *J. Phys. Soc. Jpn.* **53**, 1728 (1984).
- [7] P. J. Stiles, F. Lin, and P. J. Blennerhassett, *Phys. Fluids A* **5**, 3273 (1993).
- [8] R. J. Turnbull and J. R. Melcher, *Phys. Fluids* **12**, 1160 (1969).
- [9] I. M. Yavorskaya, N. I. Fomina, and Y. N. Belyaev, *Acta Astronaut.* **11**, 179 (1984).
- [10] J. R. Melcher, *Continuum Electromechanics* (MIT Press, Cambridge, MA, 1981).
- [11] In Eqs. (11) the mobilities b_{\pm} can be computed as $b_{\pm} = a_{\pm}/\rho\nu$ for highly insulating liquids with $a_{+} = 1.5 \times 10^{-11}$ C/m and $a_{-} = 3.0 \times 10^{-11}$ C/m. The diffusion coefficients K_{\pm} are given by the Einstein relation $K_{\pm} = k_B T b_{\pm}/q$ [10].
- [12] S. Chandrasekhar, *Hydrodynamic and Hydromagnetic Stability* (Dover, New York, 1961).
- [13] H. N. Yoshikawa, O. Crumeyrolle, and I. Mutabazi, *Phys. Fluids* **25**, 024106 (2012).
- [14] M. C. Cross and P. C. Hohenberg, *Rev. Mod. Phys.* **65**, 851 (1993).
- [15] M. C. Cross, *Phys. Fluids* **23**, 1727 (1980). The equation for τ_0 given in the present paper is different by a factor Pr^{-1} from the equation given in this reference due to the difference in the scale of time in nondimensionalization.
- [16] This correlation enables us to compare the values of the constant ℓ for the DEP and RB convections. Cross [15] has found $\ell \approx 0.70$ for the RB convection with scaling the amplitude A by the relationship $(\text{Nu} - 1)R/R_c = |A|^2$ where R is the Rayleigh number and R_c is its critical value. Applying the same scaling to the DEP convection, we have $\ell = 1/0.78 = 1.3$.
- [17] A. Schlüter, D. Lortz, and F. Busse, *J. Fluid Mech.* **23**, 129 (1965).